Stratified Deformation Space and Path Planning for a Planar Closed Chain with Revolute Joints

L. Han, L. Rudolph, J. Blumenthal, and I. Valodzin

Department of Mathematics & Computer Science, Clark University
{lhan,lrudolph,jblumenthal,ivalodzin}@clarku.edu

Abstract: Given a linkage belonging to any of several broad classes (both planar and spatial), we have defined parameters adapted to a stratification of its deformation space (the quotient space of its configuration space by the group of rigid motions) making that space "practically piecewise convex". This leads to great simplifications in motion planning for the linkage, because in our new parameters the loop closure constraints are *exactly*, not approximately, a set of linear inequalities. We illustrate the general construction in the case of planar nR loops (closed chains with revolute joints), where the deformation space (link collisions allowed) has one connected component or two, stratified by copies of a single convex polyhedron via proper boundary identification. In essence, our approach makes path planning for a planar nR loop essentially no more difficult than for an open chain.

1 Overview

Motion planning is important to the study of robotics [13, 3, 15] and is also relevant to other fields as diverse as computer-aided design, computational biology, and computer animation. A unifying concept for motion planning is the set of all configurations of a system under study, called the configuration space of the system and here denoted *CSpace*. In terms of *CSpace*, motion planning amounts to finding a valid curve connecting two given points, where a system configuration is valid if it satisfies the underlying constraints of the system—*e.g.*, the collision free constraint for rigid objects, joint limit constraints for linkage systems, and loop closure constraints for closed chains. Thus all the complexity of motion planning is encoded in *CSpace* and its partition into subsets *CFree* and *CObstacle* of valid and invalid configurations.

In many practical systems, *CSpace* has high dimension and a complicated structure in its own right. For some constraints, the partition introduces much greater complication; for instance, the fastest complete planner taking into

The authors acknowledge computing support from NSF award DBI-0320875, and thank the anonymous reviewers for their helpful comments.

account the ubiquitous collision free constraint [2] has exponential running time complexity. The general impossibility of analytically computing *CSpace* and its partition has driven the development of sampling based methods like Probabilistic Roadmap Methods (*PRM*) [11] and Rapidly-exploring Random Trees (*RRT*) [12], that try to capture the connectivity of *CSpace* or *CFree* using sampling and discrete data structures. These methods have been shown to perform very well for many difficult motion planning problems.

Knowledge of *CSpace*—hard as it is to compute—is invaluable for understanding the system in question and developing efficient motion planning algorithms. There has been renewed interest in studying and determining *CSpace* in the past few years. In particular, Trinkle, Milgram and Liu [22, 20, 18, 17] have made important discoveries for *CSpace* of a kinematic chain with fully rotatable joints, either n spherical joints in space (nS) or n revolute joints (nR) in the plane. Building on earlier work by geometers [16, 10], they obtained results on the geometry and topology of the set of closure configurations for a closed chain, initially without imposing the collision free constraint but recently allowing point obstacles. Using this information they develop complete path planners, such as an $O(n^3)$ accordion planner for a closed chain (ignoring collisions), and a planner for avoiding p point obstacles with conjectural lower and upper bounds $\Omega(p^{n-3})$ and $O(p^{2n-7})$. Their work, formulated with joint angle parameters, uses advanced topological tools.

The configuration of a multi-object system in the plane $\mathbb{R}^2$ or space $\mathbb{R}^3$ can be described by the configuration of the objects with respect to a local frame and a transformation from the local frame to a fixed reference frame. Unlike a rigid body which has fixed local coordinates for all points, a multi-body system has different local configurations. Thus a configuration of a multi-body system is described by a rigid body transformation together with a deformation of the system. Call the set of all deformations of the system its deformation space, *DSpace* for short, so that *DSpace* is *CSpace* modulo rigid motions of $\mathbb{R}^2$ or $\mathbb{R}^3$. For instance, for a kinematic chain the local coordinates of the joints are changed by deformations facilitated by the joint degrees of freedom, and restricted by constraints—*e.g.*, fixed link lengths and, for closed chains, the loop closure constraint—which are independent of rigid motions and so effectively are defined on *DSpace* of the chain. Here we focus on the *DSpace* of a loop and ignore the collision free constraint until section 3.3.

We have recently developed a new set of parameters—in this paper denoted by $\mathbf{r}$ and $\mathbf{s}$—to describe *DSpace* for many broad classes of planar and spatial linkages, including planar chains and loops with revolute joints, spatial chains and loops with spherical joints, chains with variable link lengths (which can model prismatic joints), and various kinematic structures more complicated than a chain or single loop. (Linkages can also be used to model a sequence of points under distance constraints.) Unlike the parameters used in earlier work, $\mathbf{r}$ and $\mathbf{s}$ are not joint parameters: $\mathbf{r}$ is a vector of inter-joint distances, and $\mathbf{s}$ is a vector of triangle orientation data to be described below. We use $\mathbf{r}$ and $\mathbf{s}$ to endow *DSpace* of a linkage with a stratification rendering

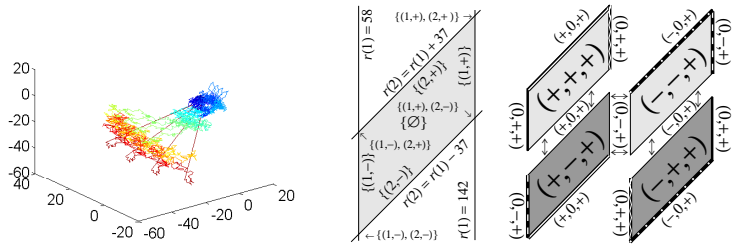

(a) A linear path for a spatial $1000S$ loop

(b) *DStretch*, and one component of *DSpace*, for a planar $5R$ loop

Fig. 1. The $5R$ loop in (b) has link lengths $(100, 42, 37, 95, 86)$.

it *practically piecewise convex* in a sense we will explain. For both planar and spatial linkages, **r** and **s** are uncoupled and **r** carries the complicated part of the "practical piecewise convexity" of *DSpace*; for planar linkages, **s** serves only to keep track of the "pieces", whereas for spatial linkages there is just one "piece" and **s** serves only to contribute extra "practically convex" dimensions.

Complete treatments of our stratification and new parameters for various linkage types—including both spatial and planar chains—will appear in our future papers. Here we describe our approach for the special but representative case of a planar nR loop, which gives an excellent indication of one major computational and conceptual advantage of our new approach, namely, how constraints (*e.g.*, closure constraints on a loop) that are highly non-linear in terms of traditional joint angle parameters become *linear inequalities* in terms of **r** and **s**. Our reformulation of the constraints and the resulting practical piecewise convexity of *DSpace* greatly simplify motion planning for both planar nR loops and spatial nS loops, as highlighted by the following examples.

Example 1. Consider the problems of generating and joining closure deformations for a loop. Fig. 1(a) illustrates a path between two deformations of a certain spatial $1000S$ loop with randomly chosen link lengths. The two ends of the path were generated by a method we call diagonal sweeping [8]. For each, we found a valid vector **r** of 997 positive inter-joint distances, and a vector **s** of 997 random angles in $[0, 2\pi]$ specifying triangle orientations (all angles are valid), in 19 milliseconds with Matlab on a desktop computer. Our space of valid vectors **r** and the cut-open 997-dimensional torus $[0, 2\pi]^{997}$ are both convex, so the path was then very easily calculated using *linear* interpolation.

Example 2. A planar nR loop has more complicated *DSpace* and path planning than a spatial nS loop. For a planar nR loop with generic link lengths, the set of feasible values of **r**, which we call *DStretch*, is an $(n-3)$-dimensional convex polyhedron, and "almost all" of *DSpace* can be reconstructed from 2^{n-2} copies of *DStretch* glued together along parts of their boundaries into either one connected component or two (depending on the number of "long links", a technical term [22]; see section 2.4); the remainder of *DSpace* is comparatively low-dimensional and does not hinder motion planning. For

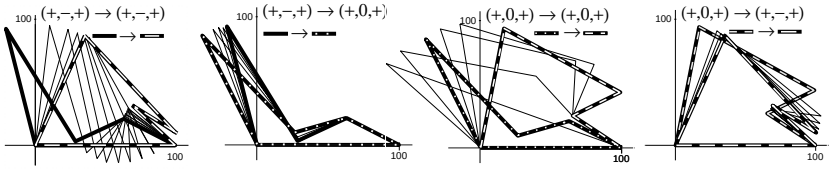

(a) A linear path (b) Segment 1 (c) Segment 2 (d) Segment 3

Fig. 2. The linear path in (a) stays in one stratum but has collisions. The 3-segment path in (b)–(d) joins the same endpoints and is collision free—segment 1 ends on the edge of one copy of *DStretch*, segment 2 crosses a second copy from one edge to its opposite (where **s** has the same value), and segment 3 returns to the first copy.

one $5R$ loop, Fig. 1(b) shows the 2-dimensional *DStretch* and one component *DSpace*, comprising four copies of *DStretch* labeled with **s**-values $(s(1), s(2), +)$ ($s(i) \in \{+, -\}$; see section 2) and joined along the indicated pairs of edges; the copies in the other component are labeled $(s(1), s(2), -)$.

Example 3. If the collision free constraint is not imposed, motion planning in *DSpace* is straightforward. Within each copy of *DStretch* the convex structure provides a unique linear path joining any given start deformation to any given goal. Fig. 2(a) illustrates this for the copy of *DStretch* labeled $(+, -, +)$ in Fig. 1(b). Passing between copies is still straightforward, although uniqueness of paths is lost—a fact which can be advantageous for motion planning. In fact, any path joining deformations on different copies of *DStretch* necessarily passes through singular deformations. In section 3, we use a notion of singularity depth (defined in section 2.3) to give upper bounds on the number of singular deformations that must traversed by a path joining two given closure deformations of a planar nR loop. There is a trade-off between the number of singular deformations traversed and their depth. Essentially, the greater the singularity depth of a deformation, the more singular the deformation; a non-singular deformation has singularity depth 0. We show that any two closure deformations in the same component can be connected by a piecewise linear path traversing at most $n - 2$ singular deformations, all of depth 1; they can also be connected via at most 2 singular deformations, one of which has singularity depth at least $n - 3$ (it is a triangle deformation generalizing one devised by Lenhart and Whitesides [16]). Importantly, the singular deformations are reusable and easily computable. For $n = 1000$, we can find 998 singular **r** values of singularity depth 1 in about 20 seconds.

To find *collision free* paths like that in Fig. 2(b-d), we have developed a preliminary probabilistic planner that makes essential use of our efficient closure deformation generation and connection methods.

The efficient algorithms and nice geometry of our approach make many more systems available for use in robot design, where inverse kinematics (closely related to closure deformation generation), motion planning, and similar kinematic issues are very important (see [5, 21]).

2 *DSpace* for a planar nR loop

2.1 The idea of a stratification

We recall a few definitions from the mathematical theory of stratifications (see [6]). Suppose X is a subset of Euclidean space $\mathbb{R}^N$. A partition S of X into subsets $M_1, \ldots, M_K$ is a stratification in case: (1) $M_i \cap M_j = \emptyset$ for $i \neq j$; (2) each M_j is a connected smooth submanifold of $\mathbb{R}^N$; and (3) for each i the closure $\mathrm{cl}(M_i)$ of M_i is itself the union of some of the M_j. Each M_i is called an S-stratum. For $(i \neq j)$, M_i and M_j are incident if $M_i \subset \mathrm{cl}(M_j)$ or $M_j \subset \mathrm{cl}(M_i)$. The dimension $\dim(X)$ of X is $\max\{\dim(M_i) \mid i = 1, \ldots, K\}$; the codimension $\mathrm{codim}(M_i)$ of M_i is $\dim(X) - \dim(M_i)$. If $\mathrm{codim}(M) = 0$ then M is an open subset of X (in the topology induced on X by $\mathbb{R}^N$); if X is connected then X is the closure of the union of the codimension-0 S-strata.

Simple but paradigmatic examples of stratifications come from convexity theory. Let $P \subset \mathbb{R}^N$ be a convex polyhedron, *i.e.*, a closed bounded subset of $\mathbb{R}^N$ that is the intersection of finitely many closed half-spaces. The dimension $\dim(P)$ of P is the dimension of the unique smallest flat (*i.e.*, translated linear subspace of $\mathbb{R}^N$) containing P; the relative interior of P is its actual (topological) interior as a subspace of that flat—equivalently, the set of all points of P not contained in a face Q of P with $\dim(Q) < \dim(P)$. The partition of P into the relative interiors of all its faces is a stratification we call the face stratification *SFace* of P. Each *SFace*-stratum Q is convex, as is $\mathrm{cl}(Q)$; P has exactly one codimension-0 *SFace*-stratum. Below we make extensive use of *SFace* for a polyhedron we associate to a planar nR loop.

2.2 New Parameters

Consider a closed chain in the plane $\mathbb{R}^2$ consisting of n rigid links with consecutive link lengths $l_j > 0$ $(j = 0, \ldots, n-1)$, connected by n revolute joints. Denote the consecutive joints of the chain by P_j, so link j is the vector P_jP_{j+1} (indices are modulo n). We call P_0 the anchor of the loop, and in general call an object "anchored" if it includes P_0. For $j = 1, \ldots, n-1$, we call the vector P_0P_j an anchored diagonal of the loop; the anchored diagonals P_0P_1 and P_0P_{n-1} are also links of the loop and thus have fixed non-zero lengths, but other anchored diagonal lengths can vary and may be 0. As illustrated in Fig. 3(a), for $j = 1, \ldots, n-2$ we denote by $\mathrm{Tri}(j)$ the anchored triangle with vertices at joints P_0, P_j, and P_{j+1}; one edge of $\mathrm{Tri}(j)$ is link j and the others are anchored diagonals. At a given point of *DSpace*, $\mathrm{Tri}(j)$ is degenerate (*i.e.*, reduces to an anchored line segment) if and only if its vertices are collinear, which can happen in two distinct ways: either $\mathrm{Tri}(j)$ has three distinct but collinear vertices, or $\mathrm{Tri}(j)$ has exactly two distinct vertices, in which case we call it doubly degenerate. (Since $l_j > 0$, $\mathrm{Tri}(j)$ cannot reduce to a point.) Note that $\mathrm{Tri}(j)$ is doubly degenerate in a given deformation if and only if one of P_j, P_{j+1} coincides with P_0, so that $\mathrm{Tri}(j-1)$ or $\mathrm{Tri}(j+1)$, respectively, is

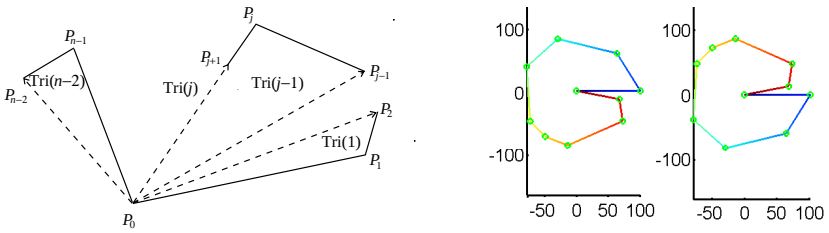

(a) Here $s(1) = s(j-1) = 1$, $s(j) = 0$, and $s(n-2) = -1$; Tri(j) is degenerate, with $r(j-1) = r(j) + l_j$.

(b) Two 10-bar deformations with opposite orientations: all $s(j)$ are $+$ at the left, $-$ at the right.

Fig. 3. New parameters and deformation examples

also doubly degenerate. We denote the subset of *DSpace* of deformations with no doubly degenerate anchored triangles by *NDD*, and its subset of deformations with no degenerate anchored triangles by *ND*.(A loop deformation that is singular in the traditional sense but includes no degenerate *anchored* triangle poses no problems for our new parametrization, so for our purposes it is non-singular. We will discuss the role of anchor choice in future papers.)

In a sense, our new parameters for *DSpace* are the triangles Tri(j) themselves, as embedded in the plane modulo a single rigid motion. We extract more conventional parameters from them as follows (see Fig. 3).

Definitions. (1) For $j = 1, \ldots, n-3$, let $r(j) = \|P_0P_{j+1}\|$; the link lengths $l_0, \ldots, l_{n-1}$ and the vector $\mathbf{r} = (r(1), \ldots, r(n-3)) \in \mathbb{R}^{n-3}$ of lengths of anchored diagonals that are not links together encode Tri$(1), \ldots,$ Tri$(n-2)$ up to unoriented congruence. The first $n-3$ of our new parameters are $r(1), \ldots, r(n-3)$. A deformation belongs to *NDD* if and only if every $r(j)$ is strictly positive. (2) For $j = 1, \ldots, n-2$, let $s(j)$ be the sign of the determinant with first column P_0P_j and second column P_0P_{j+1}; so $s(j)$ is 0 if Tri(j) is degenerate, and otherwise it is $+$ or $-$ according as the vertices P_0, P_j, P_{j+1} are oriented counterclockwise or clockwise. The last $n-2$ of our new parameters are $s(1), \ldots, s(n-2)$. Let $\mathbf{s} = (s(1), \ldots, s(n-2))$.

On *NDD*, $\mathbf{r}$ and $\mathbf{s}$ (defined throughout *DSpace*) truly are parameters.

Theorem 1 *The restriction of* $(\mathbf{r}, \mathbf{s})$*:* *DSpace* $\to \mathbb{R}^{n-3} \times \{-, 0, +\}^{n-2}$ *to NDD is one-to-one onto its image.*

Proof. Given the value of $\mathbf{r}$ on a planar nR loop with fixed link lengths $l_0, \ldots, l_{n-1}$ and no doubly degenerate anchored triangles, we first reconstruct the triangles Tri(j) abstractly. Using the value of $\mathbf{s}$ on the deformation, and starting from an arbitrary placement of Tri(1) in $\mathbb{R}^2$, we then successively lay down Tri$(2), \ldots,$ Tri$(j-2)$ in positions that are well-defined because at each step the anchored edge along which the next triangle must match up has length $r(j-1) > 0$ and the orientation sign $\mathbf{s}(j)$ determines on which side of that edge (if either) that triangle must lie. The only indeterminacy in this

construction is the initial placement of Tri(1); any two such placements differ by a rigid motion of $\mathbb{R}^2$ that is well-defined because $r(1) > 0$. □

Theorem 1 says that valid loop deformations in *NDD* correspond exactly to feasible values of $(\mathbf{r}, \mathbf{s})$. Moreover, given a feasible value of $(\mathbf{r}, \mathbf{s})$, the way we constructed the corresponding valid loop deformation makes it clear that we obtain other feasible values of $(\mathbf{r}, \mathbf{s})$ by changing an arbitrary set of non-zero entries of $\mathbf{s}$ from $+$ to $-$ or vice versa: reversing the sign of $s(j)$ corresponds to reversing the orientation of the non-degenerate triangle Tri(j) by flipping it across the anchored diagonal P_0P_j, and clearly any subset of the non-degenerate anchored triangles in a valid loop deformation can be flipped to create a new valid loop deformation—the entries of $\mathbf{s}$ are uncoupled from $\mathbf{r}$, and (for a given value of $\mathbf{r}$) from each other. We sum this up as follows.

Corollary 1 *If $r(1), \ldots, r(n-3)$, $s(1), \ldots, s(n-2)$ are the parameters of a valid deformation in NDD, then there is a valid deformation in NDD with parameters $r(1), \ldots, r(n-3)$, $\varepsilon(1)s(1), \ldots, \varepsilon(n-2)s(n-2)$ for every "triangle reorientation" function $\varepsilon\colon\ \{1, \ldots, n-2\} \to \{+, -\}$.* □

Thus the problem of understanding the topology and geometry of *NDD* breaks into two subproblems: (A) What is the topology and geometry of the set $\mathbf{r}(NDD)$? (B) How can $\mathbf{s}$ be used to recover the topology and geometry of *NDD* from $\mathbf{r}(NDD)$? We answer (A) in section 2.3 and (B) in section 2.4.

2.3 The Set of Feasible Values of r

In [9], we denoted the set $\mathbf{r}(DSpace)$ of feasible values of $\mathbf{r}$ by *DStretch*; we keep that notation, and also write $DStretch^+$ for $\mathbf{r}(NDD)$. Our proof of Theorem 1 shows that, for a given nR loop, a value of $\mathbf{r}$ is feasible (corresponds to some valid loop deformation) if and only if that value and the given link lengths allow the successful construction of the $n-2$ anchored triangles: if some entries of $\mathbf{r}$ are too big or too small, one or more anchored triangles will be impossible to construct. More precisely, from basic geometry we know that $a, b, c \geq 0$ are the side lengths of a possibly degenerate triangle if and only if $a \leq b + c$, $b \leq c + a$, and $c \leq a + b$; furthermore, the triangle is non-degenerate if and only if all three inequalities are strict. In our case, taken together these inequalities for Tri(1), …, Tri($n-2$) give an explicit description of *DStretch* in terms of the link lengths $l_0, \ldots, l_{n-1}$: it is the set of solutions $(r(1), \ldots, r(n-3))$ of the following system of linear inequalities $Ineq_j^\sigma$. (Here j indicates that Tri(j) contributed the inequality; $Ineq_j^+$ and $Ineq_j^-$ define anti-parallel half-spaces, to which that defined by $Ineq_j^+$ is perpendicular.)

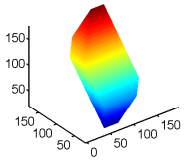

(a) *DStretch* of a certain planar $6R$ loop

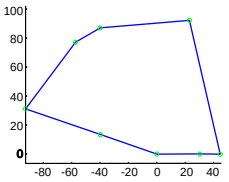

(b) Deformation of a planar $8R$ loop of singularity depth 2

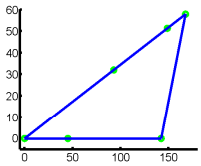

(c) The $6R$ loop in a Lenhart–Whitesides deformation

Fig. 4. The image in the 5-dimensional *DStretch* for the $8R$ loop of the deformation in (b) lies in a 3-dimensional face isometric to the polyhedron in (a).

$$\left.\begin{array}{rrl}
Ineq_j^+: & r(j)-r(j-1) \le & l_j \\
Ineq_j^-: & -r(j)+r(j-1) \le & l_j \\
Ineq_j^\perp: & -r(j)-r(j-1) \le & -l_j
\end{array}\right\} \; j=2,\ldots,n-3 \qquad (1)$$

$$\begin{array}{rrl}
Ineq_1^+: & r(1) \le & l_0+l_1 \\
Ineq_1^-: & -r(1) \le & -|l_0-l_1| \\
Ineq_{n-2}^+: & r(n-3) \le & l_{n-2}+l_{n-1} \\
Ineq_{n-2}^-: & -r(n-3) \le & -|l_{n-2}-l_{n-1}|
\end{array}$$

Rewritten in matrix format, system (1) becomes $DStretch = \{\mathbf{r} \mid T\mathbf{r} \le \mathbf{b}\}$, where $\mathbf{b} = (l_0+l_1, \ldots, -|l_{n-2}-l_{n-1}|)$ and $\le$ is applied termwise. Each row of T corresponds to an inequality $Ineq_j^\sigma$ in (1), so restricts $\mathbf{r}$ to a closed half-space; thus *DStretch* is the intersection of at most $3n-8$ closed half-spaces. The link lengths are fixed, so each $r(j)$ is bounded between zero and the sum of all link lengths. Thus *DStretch* is also bounded and is a *convex polyhedron.*

Example 4. Fig. 4(a) shows *DStretch* for a planar $6R$ loop with link lengths $(45, 97, 63, 20, 59, 98)$. It is a 3-dimensional polyhedron, with faces of codimension 0 (its interior), 1 (the interiors of its polygonal faces), 2 (the interiors of its edges), and 3 (its vertices). Since $r(1) \ge 97-45$, $r(3) \ge 98-59$, and $r(2) \ge r(3)-20 \ge 19$, (1) shows that for this loop $DStretch^+ = DStretch$. The same polyhedron also arises as the closure of a codimension-2 face of the 5-dimensional polyhedron *DStretch* of a planar $8R$ loop with link lengths $(31, 14, 97, 63, 20, 59, 56, 42)$, corresponding to deformations (like that in Fig. 4(b)) with Tri(1) and Tri(6) both degenerate.

Fig. 4(c) shows a special deformation of the $6R$ loop used in Example 4, generalized from the concept of "standard triangular form" used by Lenhart and Whitesides [16]. It is defined by finding joint index j satisfying $\sum_{i=0}^{j-1} l_i \le L/2$ and $\sum_{i=0}^{j} l_i > L/2$, where L is the sum of all link lengths, and then using the subchain from joint 0 (the anchor) to joint j, link j, and the subchain from joint $j+1$ to 0 as three sides of a (possibly degenerate) triangle. It is easy to see that the r value of such a deformation is a vertex of *DStretch*, which

we will call the *LW* vertex. We will call a deformation an *LW* deformation if the r image of the deformation is the *LW* vertex. Note that other *DStretch* vertices are also of great interest; our focus on the *LW* vertex in this paper is to facilitate the description of earlier work and illustrate the important roles of highly singular deformations in path planning.

Our earlier observations show the following.

Theorem 2 (a) *DStretch is a convex polyhedron.* (b) *DStretch*$^+$ *is the intersection of DStretch with* $\{(x_1, \ldots, x_{n-3}) \mid x_j > 0, j = 1, \ldots, n-3\}$*, and is a union of open faces of DStretch.* □

Since *DStretch* is a convex polyhedron, by section 2.1 it has a natural face stratification. As a restriction of *DStretch*, *DStretch*$^+$ also has a natural stratification: its strata are exactly those open faces of *DStretch* not contained in (and therefore disjoint from) each of the $n-3$ coordinate hyperplanes $\{(x_1, \ldots, x_{n-3}) \mid x_j = 0\} \subset \mathbb{R}^{n-3}$. For a planar nR loop that cannot have any doubly degenerate triangles, *DStretch*$^+$ = *DStretch* (see Figs. 1(b) and 2).

Each stratum Q of *DStretch*$^+$ is characterized by the set of (j, σ), denoted by $E(Q)$, for which one of the two or three linear inequalities $Ineq_j^\sigma$ in (1) associated with triangle j is replaced with the corresponding equality Eq_j^σ. (Now we can explain the labels in Figs. 1(b): they are the values of $E(Q)$ on the *DStretch* strata of the $5R$ loop.) Let $e(Q)$ be the number of elements in $E(Q)$. For a stratum in *DStretch*$^+$, $e(Q)$ is also the number of degenerate anchored triangles that can be induced by the values of $\mathbf{r} \in Q$; we call $e(Q)$ the *singularity depth* of Q. For a loop with generic link lengths, the singularity depth of a stratum Q is equal to the co-dimension of the stratum; but the singularity depth of a stratum for a loop with non-generic link lengths may be different from its co-dimension. For example, the top-left subfigure in Fig. 5 shows *DStretch* for a planar $5R$ loop with link lengths $(2, 3, 4, 2, 3)$, with its $E(Q)$ labels; two of the codimension-2 strata (the vertices where $\mathbf{r} = (1, 5)$ and $\mathbf{r} = (5, 1)$) induce three degenerate triangles and have singularity depth 3. The following results show that $E(Q)$ can be used to label the *SFace*-strata for *DStretch* and derive their incidence relations.

Theorem 3 (a) $E(Q) \neq E(Q')$ *if* $Q \neq Q'$. (b) $E(Q) \subset E(Q')$ *if* $Q' \subset \mathrm{cl}(Q)$. (c) $\mathrm{codim}(Q) \leq e(Q)$. (d) $\mathrm{codim}(Q) = e(Q)$ *if* $e(Q) \leq 1$. □

2.4 The Stratification and Topology of *DSpace*

For a stratum Q of *DStretch*, $E(Q)$ identifies which triangles, if any, are degenerate for any given $\mathbf{r} \in Q$. In other words, if $(j, \sigma) \in E(Q)$, and $\mathbf{r} \in Q$, then $\mathrm{Tri}(j)$ is degenerate in any deformation with that value of $\mathbf{r}$, forcing $s(j) = 0$ for such a deformation. On the other hand, if $(j, \sigma) \notin Q$ for any $\sigma \in \{+, -, \perp\}$, then $\mathrm{Tri}(j)$ cannot be degenerate in any deformation with that value of $\mathbf{r}$, so $s(j)$ must be $+$ or $-$ for such a deformation. This observation leads to another way to label the open face Q, namely, by an $(n-2)$-vector reflecting the

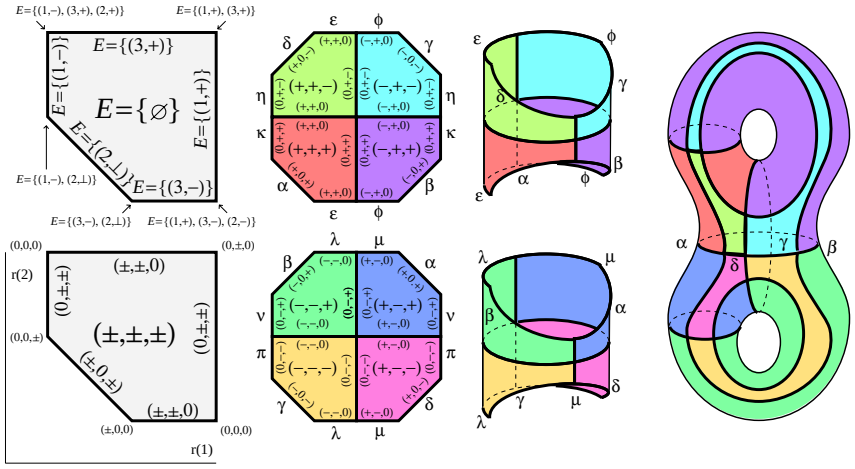

Fig. 5. *DSpace* for a planar $5R$ loop with link lengths $(2, 3, 4, 2, 3)$.

possible s values of loop deformations with $\mathbf{r} \in Q$: the j^{th} component is the symbol $\pm$ if $Tri(j)$ cannot degenerate, 0 if it must. (The bottom left sub-figure of Fig. 5 is labeled in this way.) In fact, *DStretch*$^+$ with this type of labeling can also be viewed as a compact visualization of *NDD* itself: each label is to be understood as a template in which the $\pm$-signs take on all combinations of values $+$ and $-$, and the different ways to fill in each template represent different "convex tiles" of *NDD*. From this viewpoint, each *DStretch*$^+$ stratum Q has $2^{n-2-e(Q)}$ embedded copies in *NDD* (which are the inverse images by $\mathbf{r}$), with 0 at the $e(Q)$ entries of $\mathbf{s}$ that correspond to the $e(Q)$ degenerate triangles, and $+$ or $-$ at the remaining $n-2-e(Q)$ entries that correspond to non-degenerate triangles. (Again, refer to Fig. 5 for an example.) We will show elsewhere that these embedded copies of *SFace*-strata of *DStretch*$^+$, which clearly form a partition of *NDD*, actually form a stratification (technical difficulties arise from doubly degenerate triangles, but can be overcome). We call it the "triangle orientation stratification" *STriO*.

Theorem 4 *If Q is an SFace-stratum of DStretch*$^+$*, then the STriO-strata mapped onto Q by $\mathbf{r}$ are in one-to-one correspondence via $\mathbf{s}$ with $2^{n-2-e(Q)}$, each stratum being distinguished by its unique pattern of $\{+,-\}$ orientation signs for the $n-2-e(Q)$ nondegenerate triangles.* □

The significance of Theorem 4 is that it renders *NDD*—that is, in every case "practically all" of *DSpace*, and in many cases literally all of it—*practically piecewise convex* in a strong sense: it shows how *NDD* can be decomposed *practically* into convex tiles labeled by values of $\mathbf{s}$, each of which is identified via $\mathbf{r}$ with an open face of the polyhedron *DStretch*.

As to how two *STriO*-strata can be directly joined, we have the following.

Theorem 5 *The closures of two S TriO-strata of DSpace with triangle orientation signs that differ on some set of k triangles intersect each other if and only if those triangles can become singular simultaneously.* □

For instance, on the 3-dimensional, codimension-2 *S TriO*-stratum Q for the planar $8R$ loop described in Example 4, $\mathbf{s}$ is $(0,+,+,+,+,0)$; four codimension-0 *S TriO*-strata (where $\mathbf{s}$ is $(s(1),+,+,+,+,s(6))$) are incident on Q, and a start deformation in any one of those strata can be joined to a goal in any other by a 2-segment stratum-wise linear path passing through Q as in Fig. 4(b) (or at any other point of Q).

Note that for an nR loop, if the $\mathbf{r}$ value of the LW vertex corresponds to a non-degenerate triangle, then the loop has two LW deformations with the same shape but opposite orientations. In this case, each LW deformation has singularity depth $n-3$ and connects half the convex tiles of *NDD*. If the LW triangle form degenerates into a line segment, then the loop has only one LW deformation, of singularity depth $n-2$, which connects all tiles of *NDD*.

Following [22], we say a planar nR loop ($n > 4$) has m long links provided m is the largest number for which there are link lengths $l_{j_1}, l_{j_2}, \ldots, l_{j_m}$ ($0 \leq j_1 < \cdots < j_m \leq n-1$) with the sum of any two of them being strictly greater than half the sum of all the loop's link lengths. Easily, if a loop has m long links, then $m \in \{0,2,3\}$. Prior results [16, 10] show that *DSpace* for a planar nR loop has two connected components or one, according as the loop has 3 long links or fewer. The $5R$ loops in Fig. 5 and Figs. 1(b) and 2 have 0 and 3 long links respectively; our figures show the correct reconstruction of the *DSpace* topology from the strata. Call an anchored triangle invertible if it is singular in some deformations. Such triangles are key to understanding the connectivity of *DSpace*, and lead to an alternative proof (short, but not short enough to include here!) of the *DSpace* connectivity results of [22, 16, 10].

Theorem 6 (a) *If a planar nR loop has* 0 *or* 2 *long links then every anchored triangle is invertible.* (b) *If l_{j_1}, l_{j_2} and l_{j_3} are three long links for a planar nR loop, then all but one anchored triangle is invertible, that being* $\mathrm{Tri}(j_2)$. □

3 Path Planning

3.1 Generation of Closure Deformations

We know of no prior closure deformation generation methods designed specifically for planar nR loops, though of course configuration generation methods for general closed chains [14, 7, 4, 1] apply in particular to planar nR loops. The more recent methods in [4] (random loop generator) and [1] (iterative constraint relaxation), designed with chains of many links in mind, considerably improve performance over earlier methods; but they still have difficulty for loops with many links (say, over 100), nor do they guarantee that every attempt will generate a closure deformation. Both these difficulties are overcome by using our new formulation of the loop closure constraint.

Our main task here is to compute a valid set $\mathbf{r}$ of diagonal lengths for a loop with given link lengths. Since all constraints on $\mathbf{r}$ are linear inequalities $Ineq_j^\sigma$ (or equalities Eq_j^σ, in case we wish to force $\mathbf{r}$ into particular strata of *DStretch*), we can easily find $\mathbf{r}$ with linear programming (LP). The problem size of an LP formulation for $\mathbf{r}$ is linear in n: the numbers of unknowns and constraints are both in $\Theta(n)$. Although there are as yet no theoretical bounds on the worst-case running time of LP, in practice [19] LP is considered a mature field with many efficient algorithms. We have also developed efficient methods other than LP (described in [8]) that take advantage of the kinematics of a planar nR loop and the particular simplicity of the constraints. Our fastest generation methods have linear time complexity $\Theta(n)$, which is optimal.

3.2 Connection of Closure Deformations

To the best of our knowledge, there are two complete planners for connecting deformations of a planar nR loop, ignoring collisions. The line tracking planner [16] of Lenhart and Whitesides generates a path in time $O(n)$ by using simple line tracking motions to move two given query deformations to their "standard triangle form", in two opposite orientations if needed, and then to move both triangle deformations to an appropriate singular deformation that allows the change of the triangle orientations. For some start and goal deformations, only one standard triangle form needs to be passed through. The accordion planner [22] of Trinkle and Milgram generates a smooth path between given deformation pairs and empirically exhibits cubic running time. It is also known [22, 20] that each component of *DSpace* for a planar nR loop with 3 long links is a $(n-3)$-dimensional torus parametrized by joint angles of the short links, so valid paths in a given component can be generated by linear interpolation of those angles (modulo 2π). Path planning for a planar nR loop using our new parameters is considerably simplified by the nice geometry of the *DSpace*, because (viewed through $\mathbf{r}$) all strata and their closures are convex, so two query deformations in the closure of a single stratum can be joined by a path on which $\mathbf{r}$ linearly interpolates their $\mathbf{r}$ values (or by a Manhattan path on which only one or a few entries of $\mathbf{r}$ change on each segment). If two deformations are in the same component of *DSpace* (easily checked), we can join them by a piecewise linear path once we determine critical singular deformations through which to pass successively between strata. We sum this up in the nearly self-explanatory algorithm Fig. 6, where only Step 7 may require further comment.

Briefly, there are many ways to compute critical intermediate deformations. Assume the query deformations have different orientations for k triangles. Fig. 7 illustrates one extreme: we compute k codimension-1 strata, one for each triangle that needs to be inverted, then pass through them one at a time; feasibility is guaranteed by standard facts about stratified manifolds (cf. [6]). For a planar nR loop, we need at most $n-2$ singular deformations on codimension-1 strata, one for each triangle, so our path will be piecewise

```
1. find the number and indices of the triangles, in which the two given
   deformations have opposite orientations
2. if the deformations do not have opposite orientation for any triangle
3.     pathExistence=true; criticalIntCfgs=null;
4. elseif (the loop has 3 long links) and ...
   (the two cfgs have opposite orientations for the non-invertible triangle)
5.     pathExistence=false;
6. else
7.     pathExistence=true; find critical intermediate cfgs;
8. end;
```

Fig. 6. Algorithm for Connecting Two Closure Deformations of a Planar Chain

linear with at most $n-1$ segments, each on the closure of one codimension-0 stratum. With this approach, the running time of our algorithm is determined by the time needed to generate $O(n)$ singular deformations of depth 1, and has an upper bound of $O(n^2)$ when using deformation generation methods with linear running time [8].

Alternatively, we can look for a stratum of singularity depth at least k that corresponds to those triangles and directly joins the two strata. The extreme of this approach is to use the LW deformations mentioned earlier: we can (ignoring collisions) connect *any* two query deformations of an nR loop in the same component of *DSpace* by using at most 2 critical deformations, one a LW deformation and the other a deformation singular in (at least) the unique non-singular anchored triangle (if one exists) of the LW deformation. Fig. 8(a) shows the two critical deformations (subgoals), the first subgoal being the LW deformation, as used to connect the same start and goal of a $5R$ loop

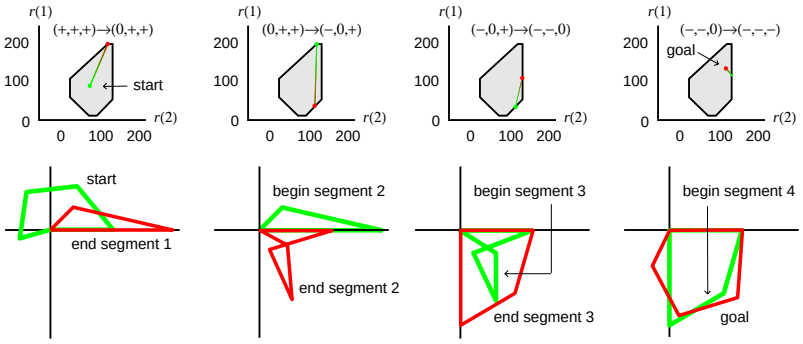

Fig. 7. Above, we show a piecewise-linear path in *DSpace* for a planar $5R$ loop link lengths $[100, 90, 80, 75, 50]$, connecting the closure deformations $(80, 70, +, +, +)$ and $(125, 110, -, -, -)$ by traversing four codimension-0 $STriO$-strata (each identified via $\mathbf{r}$ with a copy of *DStretch*, and labeled with its value of $\mathbf{s}$), crossing common boundary pieces of higher codimension. Below, we picture the loop itself, in its deformations at the beginning and end of each segment.

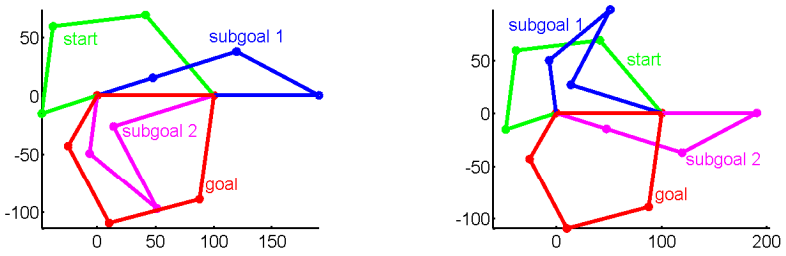

(a) path1 (b) path2

Fig. 8. Two paths for connecting the same start and goal deformations as in Fig. 7, using two singular **r** values—one the LW vertex (for the triangle deformations)—in two different orders, along with appropriate **s** values.

as in Fig. 7. Clearly the running time for generating one such path, again determined by the generation time of the two special critical deformations, is $\Theta(n)$, which is optimal.

In Fig. 8(b), the same problem as in Figs 7 and 8(a) is solved with the *LW* deformation as the second subgoal: in fact, subgoal 1 (2) in Fig. 8(a) has the same **r** value as subgoal 2 (1) in Fig. 8(b). Recall that for a loop with given link lengths, a feasible **r** value completely specifies which triangles are singular or not. Denote by $dt(\mathbf{r})$ the (possibly empty) set of the indices of the anchored triangles that are singular under the given value of the diagonal lengths **r**. So to connect two deformations in the same connected component but with opposite orientations in k triangles of indices $\{j_1, j_2, \ldots, j_k\}$, we need to find **r** values $\{\mathbf{r}_1, \mathbf{r}_2, \ldots, \mathbf{r}_m\}$, such that $\{j_1, j_2, \ldots, j_k\} \subseteq \bigcup_{i=1}^{m} dt(\mathbf{r}_i)$. For such an **r** set having m members, these **r** values can be used in arbitrary orders, along with appropriate s values; we obtain $m!$ different but related paths. An example with $m = 2$ is shown in Fig. 8.

Our connection method is clearly complete and guarantees to find a path between any two closure deformations in one connected component. The complexity of this algorithm depends on the complexity of the generation of the critical singular deformations. But we note that the singular deformations can be reused. If it is known that a large number of path planning problems will be performed for a fixed loop, it will be worth preprocessing the loop to find critical deformations, be they the *LW* deformation or deformations of lower singularity depths. Thereafter we can solve any connection problem for any two deformations in constant time $\Theta(1)$ by using the *LW* deformation, or in time $O(n)$ by picking appropriate critical singular depth 1 deformations.

3.3 Sampling-Based Collision-Free Closure Path Planning

The closure deformation connection methods just described do not consider the *collision free constraint*, so may involve interference between the links, as

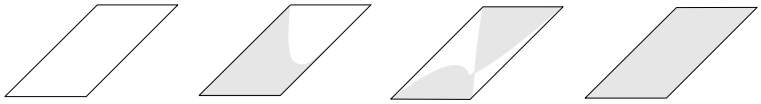

(a) $cl(S_{+++})$ (b) $cl(S_{-++})$ (c) $cl(S_{+-+})$ (d) $cl(S_{--+})$

Fig. 9. *DSpace* for the 5-bar loop with 3 long links already familiar from Fig. 2.

in Fig. 7. Extensive research by the motion planning community has made it clear that the collision free constraint is very difficult to deal with, and that it is very hard to describe *CFree* and *CObstacle* analytically for general obstacles. Recent successes of randomized path planners suggest that sampling based planners like *PRM* and *RRT* may be an important framework in which to integrate efficient node generation and connection methods (including ours and previous ones) while also dealing with such difficult factors in planning as high dimensionality and complicated linkage constraints. Our preliminary strategy has been to capture the stratum connectivity with a roadmap or trees, from which we construct the global connectivity of *DFree* and solve for paths for given query deformation pairs. Fig. 9 suggests the daunting complexity of this problem. The shaded areas are the parts of *DObstacle* in the copies of *DStretch* that make up half of *DSpace* (the other half is its mirror image). The unobstructed part of the $(+,-,+)$ stratum has two connected components, which can however be connected via the $(+,+,+)$ stratum, as in Fig. 2(b-d).

4 Summary

In this paper, we used our new parameters—some inter-joint distances and triangle orientation data—to study the stratified deformation space and efficient path planning for a plainer closed chain with revolute joints. Instead of formulating the loop closure constraint as nonlinear equations in joint angles, we break a loop into an open chain of triangles then use the triangle inequality repeatedly to formulate the constraint as a set of linear inequalities. This new formulation endows the deformation space with a nice geometry; for a generic nR loop it is a stratified space of convex strata. This geometry (and its generalizations for more complex kinematic systems) greatly simplifies kinematics related issues including the generation and connection of closure deformations. In effect, our new parameters make path planning for a planar nR loop (or a spatial nS loop) no more difficult than path planning for an open chain.

References

1. O. B. Bayazit, D. Xie, and N. M. Amato. Iterative relaxation of constraints: A framework for improving automated motion planning. In *Proc. IEEE Int. Conf. Intel. Rob. Syst.* (*IROS*), pages 586–593, Edmonton, Alberta, Canada, Aug. 2005.

2. J. Canny. *The Complexity of Robot Motion Planning*. MIT Press, 1988.
3. H. Choset, W. Burgard, S. Hutchinson, G. Kantor, L. E. Kavraki, K. Lynch, and S. Thrun. *Principles of Robot Motion: Theory, Algorithms, and Implementation*. MIT Press, 2005.
4. J. Cortes and T. Simeon. Sampling-based motion planning under kinematic loop closure constraints. In *Proc. of Workshop on Algorithmic Foundations of Robotics*, 2004.
5. J. J. Craig. *Introduction to Robotics: Mechanics and Control, 2nd Edition*. Addison-Wesley Publishing Company, Reading, MA, 1989.
6. M. Goresky and R. MacPherson. *Stratified Morse Theory*. Springer-Verlag, New York, 1988.
7. L. Han and N. M. Amato. A kinematics-based probabilistic roadmap method for closed chain systems. In *Algorithmic and Computational Robotics — New Directions* (*WAFR 2000*), pages 233–246, 2000.
8. L. Han, L. Rudolph, J. Blumenthal, and I. Valodzin. Inverse Kinematics of a Spatial Chain with Spherical Joints. Part II: Efficient Solving Methods. Submitted, 2006.
9. L. Han and L. Rudolph. Inverse kinematics for a serial chain with joints under distance constraints. In *Proc. of Robotics: Science and Systems*, Philadelphia, PA, 2006.
10. M. Kapovich and J. Millson. On the moduli spaces of polygons in the euclidean plane. *Journal of Differential Geometry*, pages 42:133–164, 1995.
11. L. Kavraki, P. Svestka, J. C. Latombe, and M. Overmars. Probabilistic roadmaps for path planning in high-dimensional configuration spaces. *IEEE Trans. Robot. Automat.*, 12(4):566–580, August 1996.
12. J. J. Kuffner and S. M. LaValle. RRT-Connect: An Efficient Approach to Single-Query Path Planning. In *Proc. IEEE Int. Conf. Robot. Autom.* (*ICRA*), pages 995–1001, 2000.
13. J. C. Latombe. *Robot Motion Planning*. Kluwer Academic Publishers, Boston, MA, 1991.
14. S. LaValle, J. Yakey, and L. Kavraki. A probabilistic roadmap approach for systems with closed kinematic chains. In *Proc. IEEE Int. Conf. Robot. Autom.* (*ICRA*), 1999.
15. S. M. LaValle. *Planning Algorithms*. Cambridge University Press, 2006. Also available at `http://msl.cs.uiuc.edu/planning/`.
16. W. Lenhart and S. Whitesides. Reconfiguring closed polygon chains in Euclidean d-space. *Discrete and Computational Geometry*, 13:123–140, 1995.
17. G. Liu and J. C. Trinkle. Complete path planning for planar closed chains among point obstacles. In *Robotics: Science and Systems*, 2005.
18. G. Liu, J. C. Trinkle, and R. J. Milgram. Toward complete motion planning for planar $3R$-manipulators among point obstacles. In *Proc. Int. Workshop on Algorithmic Foundations of Robotics* (*WAFR*), 2004.
19. D. Luenberger. *Linear and Nonlinear Programming*. Kluwer Academic Publishers, 2004.
20. R. Milgram and J. Trinkle. The geometry of configuration spaces for closed chains in two and three dimensions. *Homology Homotopy Appl.*, 2002.
21. R. M. Murray, Z. Li, and S. S. Sastry. *A Mathematical Introducation to Robotic Manipulation*. CRC Press, Boca Raton, FL, 1994.
22. J. Trinkle and R. Milgram. Complete path planning for closed kinematic chains with spherical joints. *Int. J. Robot. Res.*, 21(9):773–789, 2002.